

Investigation of Corona wind Effect on Heat and Mass Transfer Enhancement

R.Karami¹, B.Kamkari², K.Kashefi³

Abstract—Applying corona wind as a novel technique can lead to a great level of heat and mass transfer augmentation by using very small amount of energy. Enhancement of forced flow evaporation rate by applying electric field (corona wind) has been experimentally evaluated in this study. Corona wind produced by a fine wire electrode which is charged with positive high DC voltage impinges to water surface and leads to evaporation enhancement by disturbing the saturated air layer over water surface. The study was focused on the effect of corona wind velocity, electrode spacing and air flow velocity on the level of evaporation enhancement. Two sets of experiments, i.e. with and without electric field, have been conducted. Data obtained from the first experiment were used as reference for evaluation of evaporation enhancement at the presence of electric field. Applied voltages ranged from corona threshold voltage to spark over voltage at 1 kV increments. The results showed that corona wind has great enhancement effect on water evaporation rate, but its effectiveness gradually diminishes by increasing air flow velocity. Maximum enhancements were 7.3 and 3.6 for air velocities of 0.125 and 1.75 m/s, respectively.

Keywords—Electrohydrodynamics (EHD), corona wind, high electric field, Evaporation enhancement

I. INTRODUCTION

IT is well known that when air flows over a body of water, a thin layer of relatively inert air exists on the surface of water. This saturated air layer interferes with diffusion of water molecules from water surface to the bulk air flow. As the air velocity over the surface reduces thickness of saturated air layer increases and evaporation rate degrades, so any method which can disturb this boundary layer might improve evaporation rate. Applying electrohydrodynamic can enhance water evaporation substantially with producing a secondary air flow called corona wind. To practice this, a high voltage is applied between two electrodes. In this method, moist material is placed on the surface of a flat electrode. Corona wind impinges the surface of the material and disturbs the saturated air layer which leads to evaporation enhancement. When a dielectric placed in an electrostatic field, three forces act on it and are determined by eq. (1) [1].

$$\mathbf{F}_e = q_e \mathbf{E} - \frac{\epsilon_0}{2} E^2 \nabla \epsilon + \frac{\epsilon_0}{2} \nabla \left(E^2 \frac{d\epsilon}{d\rho_a} \rho_a \right) \quad (1)$$

1- Research Institute of Petroleum Industry . Energy Research center
West Blvd., Near Azadi Sports Complex Tehran Iran.(e-mail:
Karamir@ripi.ir)

2- Research Institute of Petroleum Industry . Energy Research center
West Blvd., Near Azadi Sports Complex Tehran Iran. (e-mail:
kamkarib@ripi.ir)

3- Research Institute of Petroleum Industry . Energy Research center
West Blvd., Near Azadi Sports Complex Tehran Iran.(e-mail:
kashefik@ripi.ir)

The first term on the right hand side of the equation is called Coulomb force and represents a volumetric electrostatic force which is connected with the presence of free electric charges (q_e) in a dielectric fluid. The second term results from non-uniformity of dielectric constant ($\nabla \epsilon$) in a fluid volume subjected to an electric field. The third term deals with an electrostrictive phenomenon and represents force acting on a dielectric in a non-uniform electric field. The first term of EHD forces is the main force which contributes to evaporation enhancement and single phase heat transfer augmentation [2]. The second and the third terms are important in two-phase heat transfer where differences in temperature and density cause variation in electric permittivity [3, 4].

Although several studies have demonstrated the feasibility of EHD-enhanced evaporation [5-9], some effective parameters in this technique need more studies. In this paper, effects of electric field intensity, primary air flow velocity and electrode spacing are investigated and correlations for evaporation enhancement and EHD performance are presented.

II. CORONA WIND THEORY AND VELOCITY

The electric corona discharge usually occurs when a high electric voltage is applied between two electrodes with substantially different radii of curvature. For this purpose, highly curved electrode could be needle or small diameter wire and the other electrode could be a flat plate or a cylinder. High intensity electric field in the vicinity of the sharp electrode causes air around it to break down partially and become a conductor. Under this condition air is ionized and results in a corona discharge. Corona discharge could be positive or negative. This is determined by the polarity of voltage on the sharp electrode with respect to the flat electrode. There are always very small amount of free electrons in surrounding air. In a positive corona electrons are attracted toward the corona electrode (sharp electrode) and positive ions are propelled to the flat electrode by Coulomb force. As the positive ions travel toward the flat electrode, they collide with neutral air molecules and exchange momentum. The result is an ion-drag flow from the sharp electrode to the flat one. This flow is also called corona wind or ionic wind [10]. It should be noted that the direction of corona wind flow is from the sharp electrode to the flat one regardless of its electrode polarity.

Electrode geometry used in this research was wire-plate electrodes. If it's assumed that wire electrode is located at $x=0$ and at a distance of L from the plate electrode, there

would be a very small bipolar region with a radius of x_0 formed around the wire electrode that positive and negative ions drag in opposing directions, so its contribution to a net ion-drag flow is negligible and could be eliminated from the calculations. Electric field distribution between two plate electrodes (E) is obtained from eq. (2) [11].

$$E^2 - E_0^2 = \frac{2I(x - x_0)}{Ab\epsilon_0} \quad (2)$$

In this equation E_0 , I , A , b , ϵ_0 are electric field intensity between two plate electrodes, electric current between two electrodes, area of flat electrode, ion mobility of positive ions and electric permittivity of free space, respectively.

Since average electric field between wire and plate electrode is equal to E_0 which represents a uniform electric field between two plate electrodes with a voltage and distance of V and L respectively ($E_0 = \frac{V}{L}$), equation (2) is applicable for wire-plate electrode geometry using average electric field. With assumption that complete momentum transfer from ionic space charges (q_e) to the air bulk take place, the conservation law of energy could be written as follow:

$$\frac{1}{2}\rho_a U_e^2 = \int_{x=x_0}^{x=L} q_e E dx \quad (3)$$

In this equation ρ_a is air density.

Combining equations (2), (3) and using the Gauss law ($\nabla \cdot E = \frac{q_e}{\epsilon_0}$), corona wind velocity (U_e) approximation under the wire electrode obtains:

$$U_e = \sqrt{\frac{2IL}{\rho_a Ab}} \quad (4)$$

Detailed derivation is given in [12].

III. EXPERIMENTAL SETUP AND PROCEDURE

Experimental setup used for the present study is shown schematically in Fig. 1. The main components are a rectangular wind tunnel, an air box, a blower, a personal computer, a high voltage DC power supply, two temperature/humidity data logger and a velocity vane anemometer. Wind Tunnel was made of Plexiglas with dimensions of 220×20×9.5 cm. An air box with converging section contained two series of honeycomb structures fixed in two different sections, placed at the inlet of the tunnel to produce a uniform airflow in the test section. In this study eight different air velocities (i.e. 0.125, 0.25, 0.5, 0.75, 1.0, 1.25, 1.5 1.75 m/s) were used. The air velocity in the wind tunnel was controlled using a damper with a sliding door

situated in the outlet of the blower and one could control the air speed into the test section by adjusting the opening of sliding door. Water container was mounted on the base of the wind tunnel. It was measured 70 cm long, 20 cm wide and 1 cm deep made of Plexiglas except for its base which was made of copper plate as the plate electrode. A copper wire as corona emitting electrode with the radius of 77 μm was suspended horizontally along the water surface with the same length of the water container and parallel to the air flow. In order to investigate the effect of corona wire spacing from the plate electrode on evaporation enhancement, wire to plate spacing was made adjustable (i.e. 3, 4, 5, 6 cm). In order to measure the dry bulb temperature and relative humidity of air at the outlet of wind tunnel more accurately, an orifice was located inside the wind tunnel at a distance of 45 cm down stream of water container to mix water vapor and bulk air flow. DC voltage was applied to the wire electrode using a high voltage power supply (Heinzinger PNC 40000-5) with range of 0-40 kV and 0-5 mA. Evaporation rate of water was determined by measuring dry bulb temperature and relative humidity of air at inlet and outlet sections of wind tunnel using a temperature/humidity data logger (Testo 177 H1). The velocity of air flow through the wind tunnel was measured by an anemometer (Testo 435) equipped with a vane probe at the outlet section of wind tunnel. All experiments were carried out in pairs (with and without electric field). In each experiment the air flow rate was set at a specific value. The first experiment was performed in the absence of electric field and evaporation rate was determined at presence of air flow alone. Immediately after that, the second experiment was carried out by applying of electric field and air flow simultaneously. The applied voltage was increased from corona inception voltage to a voltage close to the breakdown limit in 1 kV increments except for voltages below 10 kV that the increments were selected in 0.5 kV. The results obtained from the first experiment which was conducted in the presence of air flow alone were used as a reference in the evaluation of evaporation enhancement value by electric field. The level of water in the container was kept constant at 1 cm in all experiments. This procedure was repeated for different air velocities as well as different electrode spacings.

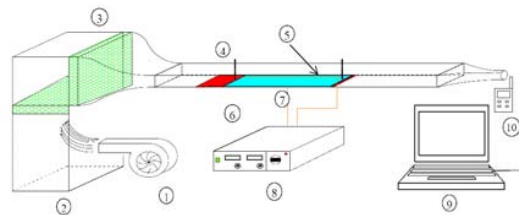


Fig. 1 The experimental set up 1. Blower 2. Air Box 3. Honeycomb 4. Wind Tunnel 5. Wire Electrode 6. Plate Electrode 7. Water Container 8. HV Power Supply 9. Computer 10. Temperature/Humidity Data logger

IV. DATA REDUCTION

As it was noted before, relative humidity and dry bulb temperature of air were measured at the inlet and outlet sections of the wind tunnel. These data were used for evaluation of humidity ratio of air (ω) using the following thermodynamic relation:

$$\omega = 0.622 \frac{\phi p_g}{p - \phi p_g} \quad (5)$$

Where ϕ is the relative humidity measured directly by the temperature/humidity data logger, p is the atmospheric pressure of air and p_g is the saturated pressure of water vapor calculated at measured temperature.

Evaporation rate was determined based on difference between the water content of inlet and outlet air flow from the wind tunnel

$$\dot{m}_{eva} = \dot{m}_{dry\ air} (\omega_2 - \omega_1) \quad (6)$$

Mass flow rate of dry air ($\dot{m}_{dry\ air}$) was obtained by measuring the mean velocity of air (U) through the wind tunnel.

$$\dot{m}_{dry\ air} = \rho_a \times U \times A_w \quad (7)$$

In this equation A_w is cross sectional area of the wind tunnel.

Sherwood number which is a dimensionless number and resembles Nusselt number in heat transfer was used to express the evaporation rate and is defined as it's conventional form:

$$Sh = \frac{h_m d}{D} = \left(\frac{\dot{m}_{eva}}{A \Delta C} \right) \frac{d}{D} \quad (8)$$

Where A is the surface area of water, the same as the plate electrode area and d is the characteristic length taken as the length of the water container. D is the mass diffusivity of water vapor into bulk air flow and it's value was found using equation (9). Mass diffusivity of water vapor is a function of air pressure (P) and temperature of water surface (T) which is equal to the wet bulb temperature of inlet air flow to the wind tunnel and is calculated based on measured dry bulb temperature and relative humidity of air at the inlet section of wind tunnel.

$$D = 2.26 \times 10^{-5} \left(\frac{101325}{P} \right) \left(\frac{T}{273.15} \right) \quad (9)$$

ΔC is the difference in water vapor concentration between the water surface and bulk air flow. The value of water vapor concentration was calculated from following relation:

$$C = \rho_a \omega \quad (10)$$

V. RESULTS AND DISCUSSION

In this paper, data obtained from the evaporation experiments are cast in the form of Sherwood number and are

presented as the ratio of Sherwood number at the presence of electric field and air flow simultaneously (Sh) to the Sherwood number at the presence of air flow alone (Sh_0). The effect of electric field on water evaporation enhancement is shown in Fig. 2, for two different air velocities (U) and four electrode spacings (L).

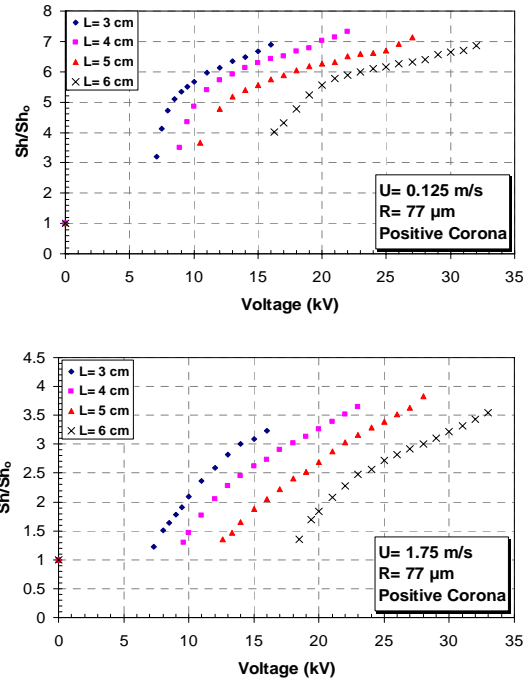


Fig. 2 Evaporation enhancement versus voltage

Although all the experiments were carried out for air flow velocities $U = 0.125, 0.25, 0.5, 0.75, 1.0, 1.25, 1.5, 1.75$ m/s, here the results are only presented for the two limiting air velocities (i.e. $U = 0.125$ and 1.75 m/s). In these figure evaporation enhancement are plotted versus applied voltage. Each plot corresponds to a fixed air flow velocity, with electrode spacing appearing as parameter.

It is shown that for all the electrode spacings, evaporation enhancement increases by increasing the applied voltage. This could be attributed to the corona wind velocity. The more the electric field strength, the more air ionization which leads to more collisions and faster corona wind. It should be noted that for a fixed air flow velocity, the maximum enhancement is nearly equal and independent of electrode spacing except for the least electrode spacing ($L = 2$ cm) which an early break down voltage inhibits further increase of voltage and reaching higher value of enhancement.

As it was expected, for a fixed voltage, lower electrode spacings show greater enhancement. This happens because of electric field intensification and increase of corona wind velocity. Also increase in electrode spacing, postpones corona inception voltage as well as break down voltage.

Moreover, if one compares the two plots in Fig. 2, it can be concluded that increase in air flow velocity leads to decrease

in the level of evaporation enhancement. To consider this behavior more accurately, the value of evaporation enhancement at different air flow velocities are compared at a fixed electrode gap in Fig. 3.

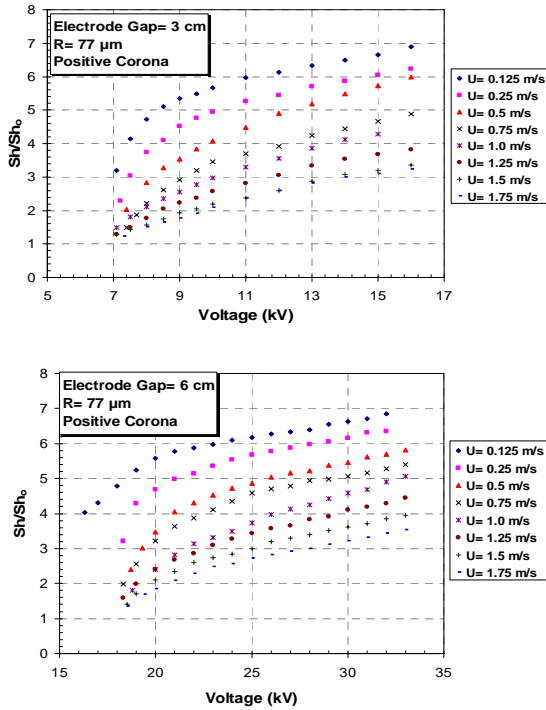


Fig. 3 Evaporation enhancement versus voltage for different air velocities

Each plot corresponds to a fixed electrode spacing, while the air flow velocity ranges from 0.125 to 1.75 m/s. Results for the two limiting electrode spacings of $L=3$ and 6 cm are presented in this figure. For both electrode spacings the effect of corona wind on evaporation enhancement was suppressed by increasing air flow velocity. In this research, the maximum enhancement ranged from 7.3 to 3.6 at $L=4$ cm, as the air velocity increased from $U=0.125$ to 1.75 m/s. It can be deduced that air flow velocity has an inverse effect on evaporation enhancement at the presence of electric field. The ions produced at the vicinity of the wire electrode are less effective in exchanging momentum to fast moving neutral air molecules than lower air velocities. Another explanation is that in high air flow velocities, saturated boundary layer over the water surface is thin and evaporation rate is already high and corona wind disturbance can not enhance evaporation rate much further, but in low air velocities, saturated layer is thick and any disturbance in this layer can lead to significant evaporation enhancement. In addition to the decrease in evaporation enhancement by increasing air flow velocity, it can be seen that at low air flow velocities, the increase in evaporation enhancement is steep and nonlinear at low voltages whereas it becomes linear at higher voltages, but as air flow velocity increases the steepness of variation of evaporation enhancement moderates gradually and becomes

nearly linear.

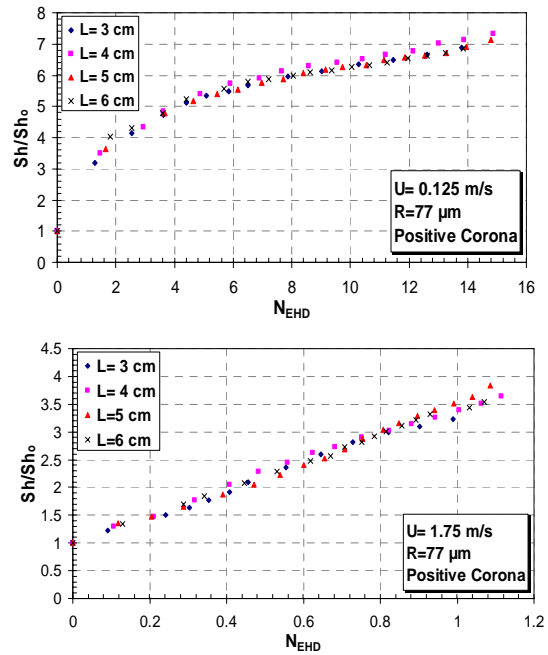


Fig. 4 Evaporation enhancement versus EHD number

The result shows that corona wind velocity as a cross flow (U_e) and axial air flow velocity (U) are two effective parameters which have a direct and inverse relationship to evaporation enhancement level, respectively, so to evaluate the enhancement in water evaporation for the cases with simultaneous presence of electric field and air flow, a dimensionless number can be defined as EHD number which is the ratio of corona wind velocity as defined in Eq. 4 to the air flow velocity.

$$N_{EHD} = \frac{U_e}{U} \quad (11)$$

The EHD number defined above is equivalent to the square root of the force ratio (Ion-drag force/ inertial force) defined by Sadek [13].

Fig. 4 shows the evaporation enhancement as a function of EHD number for two limiting air velocities $U=0.125$ and 1.75 m/s and different electrode spacings. As it was expected, in each plot for a fixed EHD number, the value of evaporation enhancement is nearly independent of electrode spacing and it is only a function of corona wind velocity. The values of evaporation enhancement for all electrode spacing and air velocities over 0.75 m/s are presented in Fig. 5. It is observed that evaporation enhancement can be very well correlated as a linear function of EHD number. In this case, the results can be correlated using following form:

$$(12)$$

$$\frac{Sh}{Sh_0} = 1 + a N_{EHD}$$

Where a is a constant determined from the correlation. In this form, the evaporation enhancement is reduced to unity when no electric field is applied and at the presence of electric field, it increases linearly with increase of EHD number. The equation of the regression line is:

$$\frac{Sh}{Sh_0} = 1 + 2.37 N_{EHD} \tag{13}$$

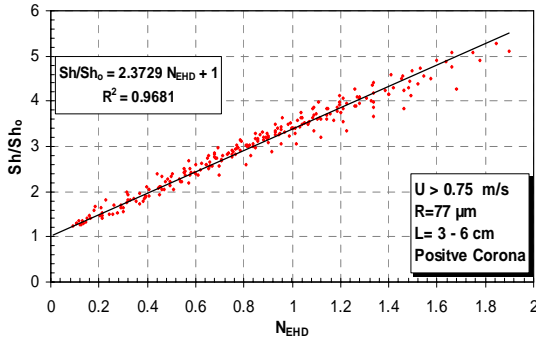


Fig. 5 Evaporation enhancement versus EHD number

Electrohydrodynamics is known as a novel low energy consumption technique which can make it as an outstanding method for increasing the rate of the heat and mass transfer. Fig. 6 shows evaporation enhancement as a function of electric power consumption for air flow velocities of $U=0.125$ and 1.75 m/s and different electrode spacings.

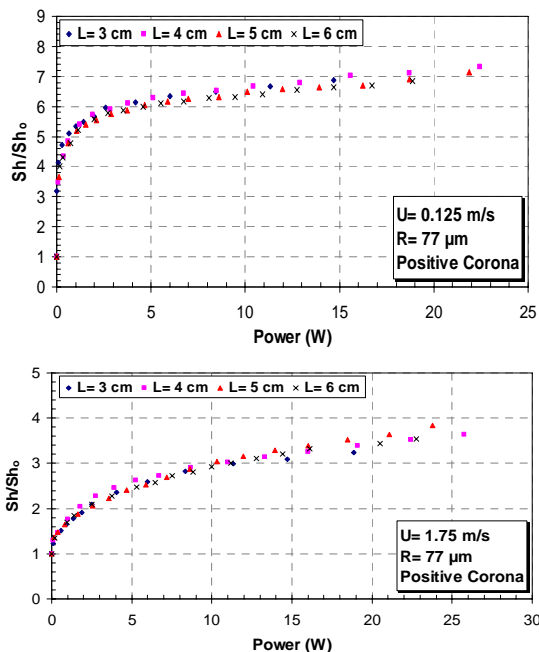


Fig. 6 Evaporation enhancement versus electrical power

Applying electric field with very small amount of energy usage can lead to great evaporation enhancement especially at low air flow velocities. For instance, at air velocity of $U=0.125$ m/s and electrode spacing of $L=3$ cm, evaporation enhancement is 3.2 by consuming 0.071 W electrical power which reduces to 1.2 as air velocity increase to 1.75 m/s. Evaporation enhancement increases steeply at low electrical powers and gently at higher electrical powers which highlights the effect of electric field at lower power consumptions. Results also show that while evaporation enhancement is a function of air flow velocity, it is nearly independent of electrode spacing for a fixed electrical power consumption. In other words, when electrical power consumption is a matter, electrode spacing is insignificant.

Performance of electrohydrodynamic technique is defined here as the ratio of increase in the heat absorbed by evaporated water at presence of electric field to the electrical power consumption (VI).

$$P_e = \frac{(\dot{m}_{eva} - \dot{m}_{eva_0})\lambda}{VI} \tag{14}$$

In this equation \dot{m}_{eva} and \dot{m}_{eva_0} are the rate of water evaporation with and without electric field, respectively. λ is the latent heat of evaporation for water. As shown in Fig. 7, performance of electrohydro-dynamic water evaporation decreases with increase of applied voltage and decrease of electrode spacing. However these results shouldn't be confused with earlier results presented in Fig. 2, which show that the evaporation enhancement increases with increase of applied voltage and decrease of electrode spacing.

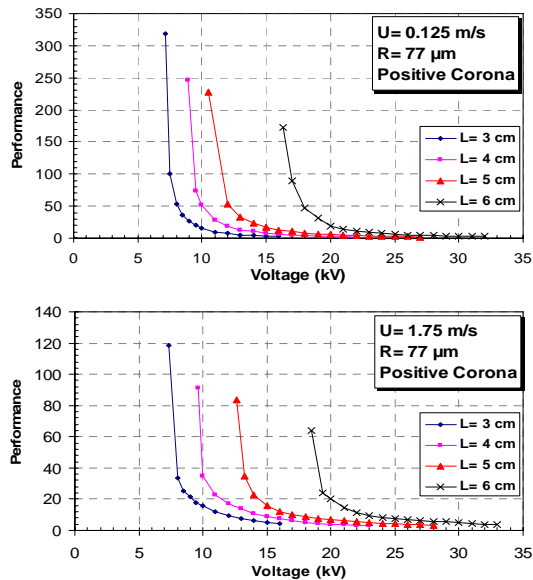


Fig. 7 EHD performance versus voltage

Fig. 7 implies that electrical energy is more effectively used at a lower applied voltage and performance falls down sharply for higher voltages. As it is seen, EHD performance value like

evaporation enhancement value is a function of both corona wind velocity and axial air flow velocity, so it seems to be possible to correlate the value of EHD performance to corona wind and axial air flow velocity. This has been performed in Fig. 8. In this figure performance values for air velocities over $U = 0.75$ m/s and different electrode spacings are plotted. As it is seen, they can be correlated very well by the following relation:

$$P_e = \frac{12.4}{(U_e^{1.4622} \times U^{0.5})} \quad U > 0.75 \text{ m/s} \quad (15)$$

According to the previous statements, this relation shows that corona wind is more effective at lower air velocities.

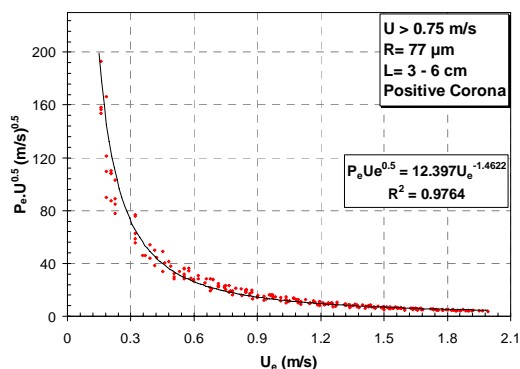


Fig. 8 EHD performance versus corona wind velocity

VI. CONCLUSIONS

This experimental research revealed the level of evaporation enhancement that can be achieved by corona wind in the wind tunnel. The effects of corona wind velocity, electrode spacing and air flow velocity on evaporation enhancement have been examined. The emitting electrode was a thin copper wire suspended above a copper plate and charged with positive DC high voltage. The results could be summarized as follow:

- The evaporation enhancement increases with increasing voltage and decreases with increasing the electrode spacing at a fixed voltage.
- It's found that as the air flow velocity over the water surface increases, EHD enhancement reduces which implies that EHD effectiveness on evaporation enhancement gradually diminishes by increasing the air flow velocity. Maximum enhancement was 7.3 obtained at air velocity of 0.125 m/s.
- It can be deduced that evaporation enhancement is nearly independent of electrode spacing at a fix corona wind velocity. This result strengthens the postulate that corona wind velocity is the main mechanism in evaporation enhancement.
- Except for very low air flow velocities, Evaporation enhancement is a linear function of EHD number.

- The performance of EHD evaporation decreases with increasing applied voltage. However this shouldn't be confused with the earlier statement that evaporation rate increases with applied voltage. What actually is emphasized here is that the electrical energy usage is more effective at a lower applied voltage
- Electrohydrodynamic technique with applying very small amount of energy can lead to a great level of enhancement, especially at voltages near to corona inception voltage.

NOMENCLATURE

A	plate electrode area (m^2)
b	positive ion mobility ($1.43 \times 10^{-4} m^2/Vs$)
C	water vapor concentration (kg_w/m^3)
T	wet bulb temperature ($^{\circ}C$)
D	mass diffusivity of water vapor (m^2/s)
d	characteristic length (m)
E	electric field intensity (V/m)
F_e	Electrohydrodynamic force (N/m^3)
h_m	mass transfer coefficient (m/s)
I	Electric current (A)
L	Electrode spacing (m)
\dot{m}_{eva}	rate of water evaporation with electric field (kg_w/s)
\dot{m}_{eva_0}	rate of water evaporation without electric field
\dot{m}_{dryair}	mass flow rate of dry air (kg_a/s)
P	atmospheric pressure (kPa)
P_e	Electrohydrodynamic performance (kg/kJ)
P_g	Saturated pressure of water vapor (kPa)
Sh	dimensionless Sherwood number
U	axial air flow velocity (m/s)
U_e	Corona wind velocity (m/s)
V	electrical voltage (V)
ρ_a	dry air density (kg_a/m^3)
q_e	free electric charges density ($1/m^3$)
ϵ_o	electric permittivity of vacuum
ω	humidity ratio (kg_w/kg_a)
ϕ	relative humidity

REFERENCES

- [1] Laohalertdechaa, S., Naphonb, P., Wongwiset, S., "A review of electrohydrodynamic enhancement of heat transfer", Renewable and Sustainable Energy Review, Vol. 11, pp. 858-876, 2007.
- [2] Molki, M., Bhamidipati, K., "Enhancement of convective heat transfer in the developing region of circular tubes using corona wind", International Journal of Heat and Mass Transfer, Vol. 47, pp. 4301-4314, 2004.
- [3] Sadek, H., Robinson, A.J., Cotton, J.S., Ching, C.Y., Shoukri, M., "Electrohydrodynamic enhancement of in-tube convective condensation heat transfer", International Journal of Heat and Mass Transfer, Vol. 49, pp. 1647-1657, 2006
- [4] Alemrajabi, A., Lai, F. C., "EHD-enhanced drying of partially wetted glass beads", Drying Technology, Vol. 23, pp. 597-60923, 2005.
- [5] Goodenough T.I.J., Goodenough P.W., Goodenough S.M. "The efficiency of corona wind drying and its application to the food industry", Journal of food engineering, Vol. 80, pp. 1233-1238, 2007.
- [6] Lai, F.C., Huang, M., Wong, D. S., "EHD-Enhanced Water Evaporation", Drying Technology, Vol. 22, pp. 595-606, 2004.

- [7] Lai, F.C., Sharma, R.K., "EHD-enhanced drying with multiple needle electrode", *Journal of Electrostatics*, Vol. 63, pp. 223–237, 2005.
- [8] Chen, Y.H., Barthakur, N.N., "Electrohydrodynamic drying of potato slabs", *Journal of Food Engineering*, Vol. 23, pp. 107–119, 1994.
- [9] Barthakur, N.N., "Electrohydrodynamic enhancement of evaporation from Nacl solutions", *Desalination*, Vol. 78, pp. 455–465, 1990.
- [10] Rashkovan, A., Sher, E., & Kalman, H. "Experimental optimization of an electric blower by corona wind", *Applied Thermal Engineering*, Vol. 22, 1587–1599, 2002.
- [11] Stuetzer, M., "Ion Drag Pressure Generation", *Journal of Applied Physics*, Vol. 30, pp. 984-994, 1959.
- [12] Kamkari, B. "Experimental Investigation of Water Evaporation Enhancement Using Electrohydro-dynamics", M.Sc. thesis, Department of Mechanical Engineering, Isfahan University of Technology, 2008.
- [13] Sadek, S., Fax, E., Hurwitz, M., "The influence of electric fields on convective heat and mass transfer from a horizontal surface under force convection", *journal of heat transfer*, Vol. 94, pp. 144-148, 1972.